

doi:10.15199/48.2022.09.59

## Deposition and optical properties investigations of WO<sub>3</sub> thin films for electrochromic device applications.

**Streszczenie.** Tungsten oxide WO<sub>3</sub> thin films are one of the most widely used layers with electrochromic properties. Various deposition methods are used to produce them, including magnetron sputtering. In this paper the authors present the construction of a Lesker high vacuum system for GLAD Magnetron Sputtering and results of optical properties investigations of WO<sub>3</sub> thin films which can be used for multilayer electrochromic systems.

**Abstract.** Cienkie warstwy tlenku wolframu WO<sub>3</sub> są jednymi z najszerzej stosowanych warstw o właściwościach elektrochromowych. Do ich wytwarzania stosowane są różne metody osadzania, w tym rozpylanie magnetronowe. W niniejszej pracy autorzy przedstawiają budowę wysokopróżniowego systemu firmy Lesker do rozpylania magnetronowego GLAD oraz wyniki badań właściwości optycznych cienkich warstw WO<sub>3</sub>, które mogą być stosowane w wielowarstwowych układach elektrochromowych.. (Depozycja oraz badanie właściwości optycznych warstw WO<sub>3</sub> do zastosowań w urządzeniach elektrochromowych).

**Keywords:** electrochromism, tungsten oxide thin films, magnetron sputtering, optical properties

**Słowa kluczowe:** elektrochromizm, warstwy tlenku wolframu, rozpylanie magnetronowe, właściwości optyczne

### Introduction

Electrochromic devices (ECDs), due to their ability to control the transmission, absorption or reflection of light, have attracted considerable interest in research and commercial applications [1]. Over the years, academia as well as industry has made a number of innovations to popularize and widely use ECD's. Nowadays, multilayer ECD systems are increasingly used as smart windows [2,3], information displays [4,5], in the automotive industry as rear-view mirrors [6,7] or sunroofs [8,9], in aviation to replace traditional glass windows and as fashionable gadgets in the form of sunglasses [9,10]. A typical multilayer electrochromic system is composed of six layers [11,12]: S / TCO / EF / FIC / ISF / TCO, where: S constitutes substrate, TCO - transparent conducting oxide, EF - electrochromic film, FIC - fast ionic conductor and ISF - ion storage film. The layer which is responsible for the color change and thus the transmission through the system is EF. A variety of materials can be used as electrochromic films, ranging from metal oxides (i.e. WO<sub>3</sub>, MoO<sub>3</sub>, IrO<sub>2</sub>, TiO<sub>2</sub>, or NiO) to organic materials (i.e. SmPc2, EuPc2, or YbPc2). One of the most effective in use is tungsten oxide WO<sub>3</sub> because it strongly absorbs visible and near-infrared light in its colored state.

This paper presents the optical and structural results of a tungsten oxide WO<sub>3</sub> thin films with four thicknesses: 40 nm, 90 nm, 120 nm and 160 nm deposited by GLAD Magnetron Sputtering.

### Materials and Methods

A GLAD Magnetron Sputter manufactured by Kurt J. Lesker Company, shown in Figure 1, was used to deposit tungsten oxide (WO<sub>3</sub>) thin films. A medium frequency 80kHz power supply was used to power the magnetron. Appropriately prepared glass substrates were placed on a rotating disk located in the centre of the chamber, parallel to the target. A two-stage pumping system, consisting of a rotary pump and a LEYBOLD TURBOVAC 360 turbo molecular pump, was used to achieve a high vacuum. The deposition process was carried out on substrates heated up to 400°C by heater power supplies UHV Design. The processes were carried out in a technological mixture of Ar and O<sub>2</sub> supplied by a mass flow metre system controlled by a Multi Gas Controller 647B by MKS Instruments. INFICON

sensors were used to control the obtained vacuum. Process parameters are presented in Table 1.

Table 1. Process parameters

Layer thickness [nm]	Time [min]	$p$ [mbar] x 10 <sup>-2</sup>	Ar flow [sccm]	O <sub>2</sub> flow [sccm]	Temp [°C]	Power supply [W]
40	20	1,95	18	2	400	50
90	47	1,95	18	2	400	50
120	59	1,96	18	2	400	50
160	88	1,97	18	2	400	50

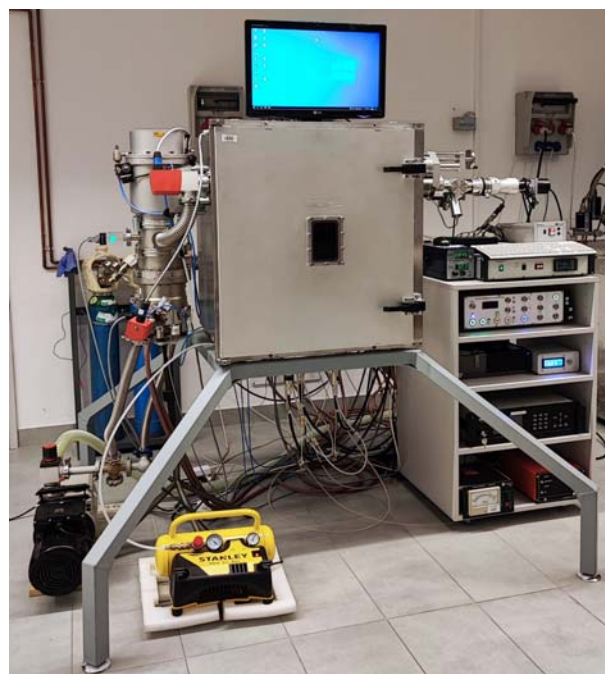


Fig. 1. GLAD magnetron sputtering system used in deposition WO<sub>3</sub> layers

In order to study the thickness of the layers obtained, a contact profilometer was used, as well as, in turn, a spectroscopic ellipsometer J.A. Woollam M-2000 and Philips X'PERT MPD X-ray diffractometer (XRR method). The homogeneity of parameters such as layer thickness and optical parameters i.e. refractive index ( $n$ ) and

extinction coefficient ( $k$ ) over the entire surface of the layers was also investigated by using spectroscopic ellipsometer J.A. Woolam M-2000 and dedicated software CompleteEASE. Transmission and absorption investigations were carried out by AVANTES AvaSpec-ULS-RS-TEC spectrophotometer.

In order to identify the layers obtained, XRD structural tests were carried out on an X-ray diffractometer Philips X'PERT MPD and then the results were analysed and interpreted using the X'PERT Data Viewer and HighScore software.

## Results

Layer thicknesses were measured using three independent methods: contact profilometry, XRR and spectroscopic ellipsometry. The XRR measurement and theoretical fit results are shown in Figure 2 for a 90nm and 120nm thin films. For both layers, the graphs show interference, which is indicative of low layer thickness. Based on these, a fitting can be made to estimate the thickness of the resulting layer. This analysis was performed for each of 4 fabricated layer. The fitting results showed very good agreement with measurements obtained on a contact profilometer.

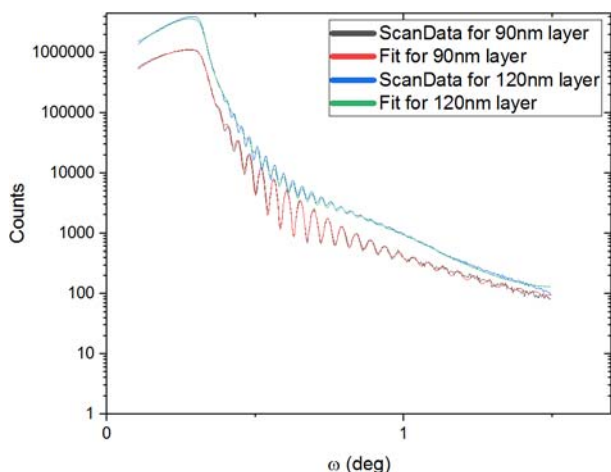


Fig. 2. Comparison of XRR results for thickness of 90nm and 120nm.

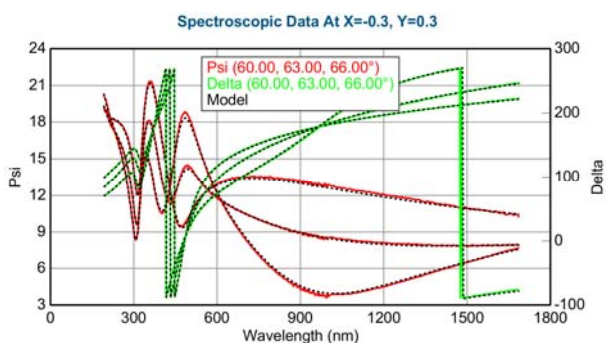


Fig. 3. Graph of wavelength dependence of Psi and Delta angles for 120nm  $WO_3$

Using the data obtained from the spectroscopic ellipsometer tests, homogeneity maps of the surface thickness for all 4 layers were made. The layers are characterized by low roughness and satisfactory homogeneity with a percentage standard deviation <4%. Measurement by spectroscopic ellipsometry is a two-step method. The first stage consists in measuring the ellipsometric angles Psi and Delta shown in Figure 3. The second stage consists in fitting a theoretical model to the obtained experimental data (the model in the form of a

dotted line is shown in Fig. 3). On the basis of model data analysis it is possible to determine the thickness of deposited layers and the values of their optical constants.

Layer thicknesses resulting from fitting of XRR results, the average layer thicknesses from spectroscopic ellipsometry are shown in Table 2.

Table 2. Comparison of thickness measured by three different measuring techniques

	Layer 1 [nm]	Layer 2 [nm]	Layer 3 [nm]	Layer 4 [nm]
Contact profilometer	40	85	120	160
Layer thicknesses resulting from fitting of XRR results	37,2	89	119,6	159,7
Average layer thickness from ellipsometric studies	42,13	91,97	121,29	161,10

The method of spectroscopic ellipsometry can also be used to determine spatial maps of measured parameters. This requires the ellipsometer to be equipped with collimators to focus the optical beam up to a diameter of 140 micrometers and an analysis program to measure parameters over the entire sample surface at defined points. Example homogeneity maps for 40nm and 90nm thin films are presented in Figures 4 and Figure 5 respectively. The spectroscopic ellipsometry studies confirmed the results of previous thickness studies, showing good agreement between the results obtained.

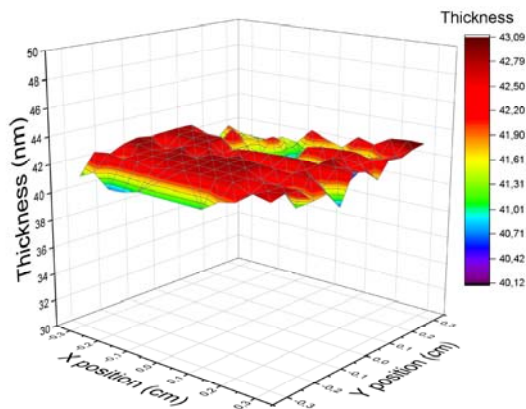


Fig. 4. 3D map of thickness homogeneity for 40nm  $WO_3$

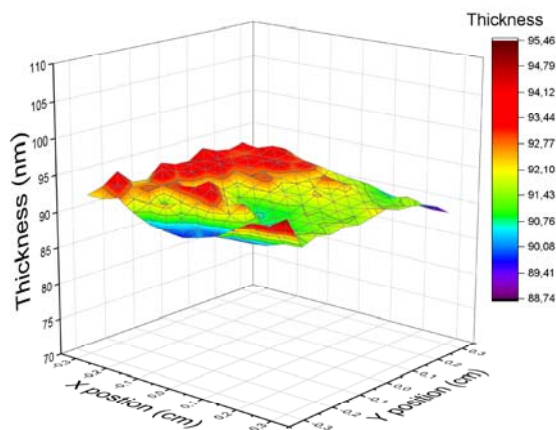


Fig. 5. 3D map of thickness homogeneity for 90nm  $WO_3$

Analysis of ellipsometric data also enables the determination of the wattages of optical constants and their distribution on the sample surface in both 2D and 3D. Homogeneity maps of the following optical constants: refractive index ( $n$ ) and extinction coefficient ( $k$ ) for a 160nm thick sample at 700 nm wavelength are shown in Figure 6 and Figure 7. They show good homogeneity of the parameters over the whole examined surface, which translates into maintenance of uniform optical parameters during the transition to the colored state.

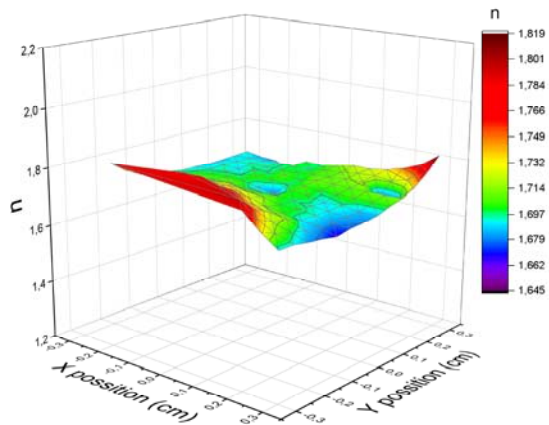


Fig. 6. 3D map of refractive index ( $n$ ) homogeneity for 160nm  $\text{WO}_3$

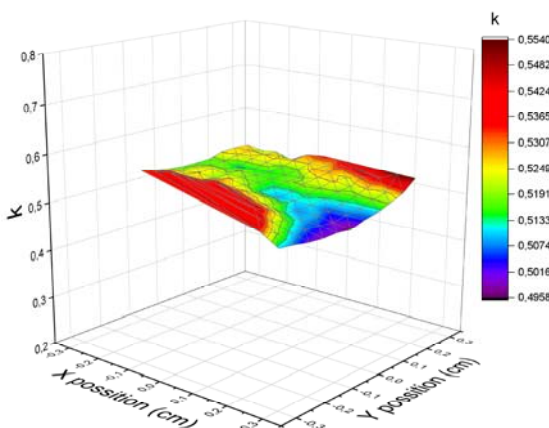


Fig. 7. 3D map of extinction coefficient ( $k$ ) homogeneity for 160nm  $\text{WO}_3$

The results of investigations of light transmission through the produced  $\text{WO}_3$  layers in the bleached state are presented in Figure 8. The layers of thicknesses 40nm, 90nm, 120nm, and 160nm are transparent in the whole wavelength range for the visible light, which translates into the possibility to use the obtained layers for the purpose of producing an electrochromic multilayer system. The lowest transmission was observed for the 160nm layer thickness and is 62% at  $\lambda=380\text{nm}$ . The 40nm thin film shows a different transmission spectrum due to its amorphous structure.

The x-ray diffraction method was used to study the phase composition of the films obtained. For 120nm and 160nm thick layers the models were fitted with which the material was identified as crystalline tungsten oxide  $\text{WO}_3$  with monoclinic structure, opening angles  $\text{Alpha} = 90^\circ$ ,  $\text{Beta} = 90.9^\circ$ ,  $\text{Gamma} = 90^\circ$ , space group  $\text{P}21/\text{n}$  and group number 14. The calculated density was  $7.3 \text{ g/cm}^3$ . For the 90nm thick layer, small peaks are seen around the angle of  $2\theta = 23^\circ$ , which indicates the fine crystalline structure of this layer. In the case of the 40nm thick layer, no Bragg

maxima originating from crystallites are noticeable, but only a broad increase in the signal, which indicates the amorphous [13] character of the obtained tungsten oxide layer. Figure 9 presents diffraction patterns collected for an omega angle of  $0.5^\circ$ , with identified Miller indices for a  $\text{WO}_3$  layer of 160nm thickness.

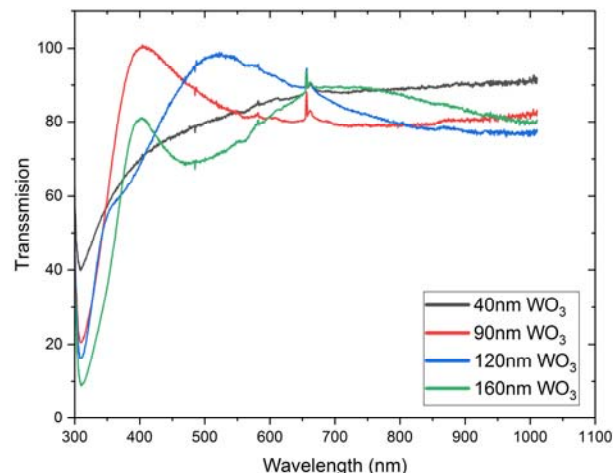


Fig.8. Transmission wavelength dependence diagrams for  $\text{WO}_3$  thin films with thicknesses of 40nm, 90nm, 120nm, 160nm.

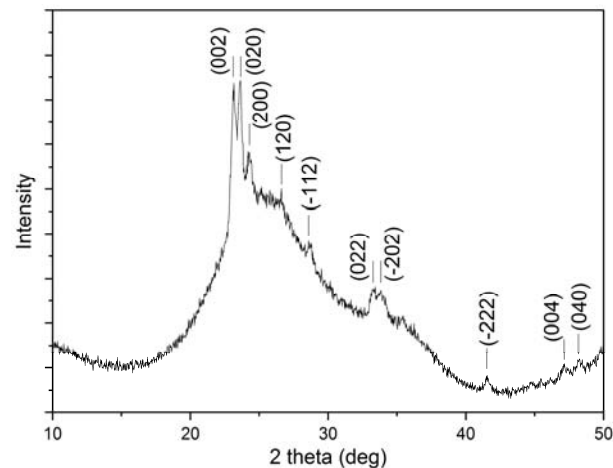


Fig. 9. XRD diffraction patterns with Miller's indices for 160nm  $\text{WO}_3$  thin film

Table 3 presents a summary of the intensities of the determined peaks as a function of the  $2\theta$  angle for the values determined from the measurement with the data base values, together with the Miller indices corresponding to the peak.

Table 3. Comparison of measured values with data base values of the intensities of the determined peaks

Measured value		Data base value		h	k	l
$2\theta$	Intens. [%]	$2\theta$	Intens. [%]			
23,112	100	23,147	100	0	0	2
23,584	96	23,612	78,3	0	2	0
24,271	33,4	24,37	97,3	2	0	0
26,584	11,3	26,619	15,2	1	2	0
28,665	9,8	28,643	16	-1	1	2
33,224	19,6	33,303	49,9	0	2	2
33,689	12,5	33,585	23,8	-2	0	2
41,477	6,3	41,467	15,9	-2	2	2
47,101	7,3	47,312	8,7	0	0	4
48,169	7,5	48,308	8,7	0	4	0

## Conclusions

Tungsten oxide WO<sub>3</sub> layers were obtained by GLAD Magnetron Sputtering process. X-ray phases of WO<sub>3</sub> with monoclinic structure were identified. The thickness of the layers was determined using three independent methods (contact profilometry, XRR, spectroscopic ellipsometry). The obtained layers are characterized by low roughness and homogeneity of thickness and optical constants. This is presented in the form of thickness uniformity maps and optical constants. Tungsten oxide WO<sub>3</sub> layers are the main element of multilayer electrochromic systems, which are coloured when a small voltage is applied. The resulting layers, in the bleached state, are characterized by high transmission in the visible light range, which has been confirmed by transmission studies. This is an important element in tinting/bleaching processes in order to obtain a high contrast of the two states.

**Authors:** mgr inż. Janusz Rybak, Electronics Institute, AGH University of Science and Technology, Mickiewicza 30 Ave., 30-059 Kraków, Poland, E-mail: [rybak@agh.edu.pl](mailto:rybak@agh.edu.pl); dr hab. inż. Konstanty Marszałek prof. AGH, Electronics Institute, AGH University of Science and Technology, Mickiewicza 30 Ave., 30-059 Kraków, Poland, E-mail: [marszalek@agh.edu.pl](mailto:marszalek@agh.edu.pl)

## REFERENCES

1. Wang, Z.; Gong, W.; Wang, X.; Chen, Z.; Chen, X.; Chen, J.; Sun, H.; Song, G.; Cong, S.; Geng, F.; et al. Remarkable Near-Infrared Electrochromism in Tungsten Oxide Driven by Interlayer Water-Induced Battery-to-Pseudocapacitor Transition. *ACS Applied Materials and Interfaces* (2020), 12, 33917–33925, doi:10.1021/acsami.0c08270.
2. Niklasson, G.A.; Granqvist, C.G. Electrochromics for smart windows: Thin films of tungsten oxide and nickel oxide, and devices based on these. *Journal of Materials Chemistry* (2007), 17, 127–156, doi:10.1039/b612174h.
3. Cheng, W.; Moreno-Gonzalez, M.; Hu, K.; Krzyszkowski, C.; Dvorak, D.J.; Weekes, D.M.; Tam, B.; Berlinguette, C.P. Solution-Deposited Solid-State Electrochromic Windows. *iScience* (2018), 10, 80–86, doi:10.1016/j.isci.2018.11.014.
4. Wang, Y.; Wang, S.; Wang, X.; Zhang, W.; Zheng, W.; Zhang, Y.M.; Zhang, S.X.A. A multicolour bistable electronic shelf label based on intramolecular proton-coupled electron transfer. *Nature Materials* (2019), 18, 1335–1342, doi:10.1038/s41563-019-0471-8.
5. Moon, H.C.; Kim, C.; Lodge, T.P.; Frisbie, C.D. Multicolored , Low Power , Flexible Electrochromic Devices Based on Ion Gels Multicolored , Low Power , Flexible Electrochromic Devices Based on Ion Gels. *ACS Applied Materials & Interfaces* (2016), 8, 6252–6260, doi:10.1021/acsami.6b01307.
6. Kun Wang, Kai Tao, Ran Jiang, Hongliang Zhang, Lingyan Liang, Junhua Gao, H.C. A Self-Bleaching Electrochromic Mirror Based on Metal Organic Frameworks. *Materials* (2021), 14, 1–8, doi:https://doi.org/10.3390/ma14112771.
7. Rosseinsky, D.R.; Mortimer, R.J. Electrochromic systems and the prospects for devices. *Advanced Materials* (2001), 13, 783–793, doi:10.1002/1521-4095(200106)13:11<783::AID-ADMA783>3.0.CO;2-D.
8. Sequeira, C.A.C.; Santos, D.M.F. Introduction to polymer electrolyte materials. *Polymer Electrolytes: Fundamentals and Applications* (2010), 3–61, doi:10.1533/9781845699772.1.3.
9. Da Rosa, H.B.; Ando Junior, O.H.; Furtado, A.C.; Spacek, A.D.; Bilessimo, L.D.; Malfatti, C.F.; Santana, M.V.. de Study on the Potential Use of Electrochromic Materials for Solar Energy Harvest in Brazil Market. *Renewable Energy and Power Quality Journal* (2016), 561–567, doi:10.24084/repqj14.394.
10. Chao, M.; Taya, M.; Xu, C. Smart Sunglasses Based on Electrochromic Polymers. *Polymer Engineering and Science* (2008), 48, 2224–2228, doi:DOI:10.1002/pen.21169.
11. Marszałek, K.W.; Swatowska, B. Ionic conductor for electrochromic devices. In Proceedings of the 36th International Microelectronics and Packaging IMAPS-CPMT Poland At: Kołobrzeg, 26–29 September, 2012; (2012).
12. Wroblewski, G.; Kielbasinski, K.; Stapinski, T.; Jaglarz, J.; Marszałek, K.; Swatowska, B.; Dybowska-Sarapuk, L.; Jakubowska, M. Graphene platelets as morphology tailoring additive in carbon nanotube transparent and flexible electrodes for heating applications. *Journal of Nanomaterials* (2015), doi:10.1155/2015/316315.
13. Zarzycki, A.; Dyndał, K.; Sitarz, M.; Xu, J.; Gao, F.; Marszałek, K.; Rydosz, A. Influence of GLAD Sputtering Configuration on the. *Coatings* (2020), 10, 1–14.